Published in Electric Power Systems Research, vol. 178, january 2020, article no. 106047, which should be cited to refer to this work.

DOI: https://doi.org/10.1016/j.epsr.2019.106047

Elsevier Editorial System(tm) for Electric Power Systems Research

Manuscript Draft

Manuscript Number: EPSR-D-19-00596R2

Title: On the Influence of the Soil Stratification and Frequency-Dependent Parameters on Lightning Electromagnetic Fields

Article Type: VSI:ICLP 2018

Keywords: Frequency-Dependent Soil model; Return Stroke; Distant Electric Fields; Horizontal Stratified Soil

Corresponding Author: Mr. Quanxin Li,

Corresponding Author's Institution: School of Electrical Engineering and Automation, Wuhan University

First Author: Quanxin Li

Order of Authors: Quanxin Li; Marcos Rubinstein; Jianguo Wang; Li Cai; Mi Zhou; Yadong Fan; Farhad Rachidi

Manuscript Region of Origin: CHINA

Abstract: We present an analysis of lightning electromagnetic fields taking into account the soil stratification and frequency dependence of its electrical parameters. Two current waveforms corresponding to typical first and subsequent return strokes are considered for the analysis. Different cases for the soil (homogeneous, 2-layer, frequency-dependent/constant electrical parameters) are considered. The analysis is carried out considering different distance ranges: close (50 m), intermediate (5 km) and distant (100 km). The obtained results confirm that the vertical electric field and the azimuthal magnetic field at close range can be evaluated assuming the ground as a perfectly conducting plane. The impact of the soil stratification and frequency-dependent parameters on the vertical electric field and azimuthal magnetic field appear at intermediate and distant ranges. On the other hand, the horizontal electric field is found to be very sensitive to the ground stratification for all the considered distance ranges. However, at close range, the impact of the soil becomes less significant for observation points that are located at above-ground heights of 10 m or higher.

On the Influence of the Soil Stratification and Frequency-Dependent Parameters on Lightning Electromagnetic Fields

Quanxin Li[1,2], Marcos Rubinstein[3], Jianguo Wang[1], Li Cai[1], Mi Zhou[1],Yadong Fan[1], Farhad Rachidi[2] *

[1] School of Electrical Engineering and Automation, Wuhan University, Wuhan 430072, China

[2] Electromagnetic Compatibility Laboratory, Swiss Federal Institute of Technology (EPFL), Lausanne 1015, Switzerland

[3] University of Applied Sciences of Western Switzerland (HES-SO), 1400 Yverdon-les-Bains, Switzerland
* Corresponding author. E-mail address: farhad.rachidi@epfl.ch.

Abstract—We present an analysis of lightning electromagnetic fields taking into account the soil stratification and frequency dependence of its electrical parameters. Two current waveforms corresponding to typical first and subsequent return strokes are considered for the analysis. Different cases for the soil (homogeneous, 2-layer, frequency-dependent/constant electrical parameters) are considered. The analysis is carried out considering different distance ranges: close (50 m), intermediate (5 km) and distant (100 km). The obtained results confirm that the vertical electric field and the azimuthal magnetic field at close range can be evaluated assuming the ground as a perfectly conducting plane. The impact of the soil stratification and frequency-dependent parameters on the vertical electric field and azimuthal magnetic field appear at intermediate and distant ranges. On the other hand, the horizontal electric field is found to be very sensitive to the ground stratification for all the considered distance ranges. However, at close range, the impact of the soil becomes less significant for observation points that are located at above-ground heights of 10 m or higher. It is shown that the three field components are affected more markedly by the soil stratification than by the frequency dependence of its electrical parameters, especially for intermediate and distant ranges (i.e., 5 km and 100 km). Furthermore, subsequent return stroke fields are more significantly affected by the soil stratification and frequency-dependence compared to first return stroke fields. The impact of the frequency-dependent soil parameters on the considered field components is more noticeable in a poorly conducting soil compared to a good conducting soil. We present also a comparison between simulation results with simultaneous measurements of current and distant vertical electric fields associated with rocket-triggered lightning flashes. It is shown that the computed vertical electric field waveforms for the case of a two-layer soil follow to a much better extent the corresponding experimental waveforms compared a non-stratified ground model. The frequency-dependence of the soil affects slightly the early-time response of the field. However, the late-time response of the field is essentially determined by the soil stratification.

Index Terms—: Frequency-Dependent Soil model; Return Stroke; Distant Electric Fields; Horizontal Stratified Soil

1. Introduction

The electromagnetic fields from lightning, including vertical electric field and azimuthal magnetic field, serve as an important input to the nowadays-widespread lightning location systems [1], which provide information on the discharge type, position of the strike, and estimates of the return-stroke peak currents. Furthermore, various field components serve as inputs to the so-called field- to- transmission line coupling models ([2]-[7]) adopted to evaluate unwanted lightning-induced signals on power and telecommunications networks.

Among the parameters affecting the lightning radiated electromagnetic fields, the soil is certainly one of the most important ones. In lightning-related studies, the soil has been modeled as either homogenous (e.g.,[8]-[11]), horizontally stratified (e.g., [12]-[21]), mixed path half-space (e.g.,[22]-[23]), or as irregular terrain (e.g., [24])). In all these studies, the soil electrical parameters have been assumed as constant and independent of frequency. However, it is a well-known fact that the soil conductivity and permittivity are affected not only by the soil heterogeneous structure, but also by its water content, and they exhibit frequency dependence [25]-[26].

In the past decades, several soil models have been proposed using either field or laboratory measurements. A comprehensive comparison of the soil models can be found in [27]. The effect of the frequency dependence of soil parameters has been considered recently in different studies related to lightning-induced voltages (e.g., [28]-[31]), grounding systems (e.g., [32]-[34]), above-ground and underground lightning electromagnetic fields (e.g., [25], [31]) radiated electric fields from lightning strikes to tall towers (e.g., [35]), and induced currents in overhead lines and buried cables (e.g., [36]). In all these studies, the soil was considered as homogenous. Recently, using simultaneously measured data of current and distant fields associated with triggered lightning, Li et al. [37] showed that a two-layer soil model allows to reproduce the fine structure and late time features of the distant fields to a much better extent than a homogenous soil.

In this study, which is an extended version of [38], we present an analysis of lightning electromagnetic fields taking into account both, the soil inhomogeneity (stratified soil) and the frequency dependence of its electrical parameters. The paper is organized as follows. Section II briefly presents the adopted computational models. The simulation results for the vertical and horizontal electric fields, and for the azimuthal magnetic field can be found in Section III. Section IV contains a comparison with simultaneous observations of current and distant electric field associated with triggered lightning. The paper ends with general conclusions given in Section V.

2. Computational models

2.1 Return Stroke Model

The MTLE model [39], [40] was adopted for the analysis. The channel height was assumed to be H=7.5 km. The current decay constant, λ, along the channel was assumed to be 2 km and a return stroke speed of 1.5×10^8 m/s was adopted in all the simulations. The channel-base current was represented using Heidler's functions [41]. The first return-stroke channel-base current is characterized by a peak value of 30 kA and a maximum steepness of 12 kA/μs, whereas the subsequent return stroke current has a peak value of 12 kA and a maximum steepness of 40 kA/μs [42]. The parameters of the input currents used in the simulations are given in Table I.

TABLE I PARAMETERS OF THE INPUT CURRENT FROM [42]

	I_{01} (kA)	τ_{11} (μs)	τ_{12} (μs)	n_1	I_{02} (kA)	τ_{21} (μs)	τ_{22} (μs)	n_2
First Stroke	28	1.8	95	2	-	-	-	-
Subsequent Stroke	10.7	0.25	2.5	2	6.5	2	230	2

TABLE II WATER CONTENT (WC) OF THE TWO-LAYER GROUND

Soil	Top Layer	Lower Layer	Case
Homogenous	2.6%		Case1
	11.6%		Case2
Stratified	2.6%	11.6%	Case3
	11.6%	2.6%	Case4

2.2 Frequency-Dependent Soil Model

Based on Scott's data [43]-[45], Messier [46] proposed a model, modified later by the same researcher in [47], in which the frequency-dependent soil parameters are expressed as

$$\varepsilon_r(f) = \frac{\varepsilon_\infty}{\varepsilon_0}\left(1+\sqrt{\frac{\sigma_{DC}}{\pi f \varepsilon_\infty}}\right) \quad (1)$$

$$\sigma(f) = \sigma_{DC}\left(1+\sqrt{\frac{4\pi f \varepsilon_\infty}{\sigma_{DC}}}\right) \quad (2)$$

where

$$\sigma_{DC} = 8\times10^{-3}(P/10)^{1.54}(S/m) \quad (3)$$

$$\varepsilon_\infty = 8\varepsilon_0(F/m) \quad (4)$$

in which P is the percent water content of the soil.

In this model, the conductivity measured at low frequency, σ_{DC}, is assumed to be a function of the percent volumetric water content. The high frequency limit of the dielectric constant ε_∞ is set to 8 times of permittivity of free space, ε_0. The use of this model for grounding applications was first discussed by Grcev [48]. The model has been shown to satisfy the Kramers-Kronig relationship ensuring causality [27]. Other similar models describing the soil frequency dependent parameters are also available. A thorough discussion and comparison can be found in [27].

The behavior of the relative permittivity and conductivity for homogenous soils with 2.6% and 11.6% of water content (WC) are shown in Fig. 1.

Fig. 2 shows the geometry corresponding to a two-layer soil. The top layer is characterized by a vertical depth h1 and electrical parameters ε_{r1} and ε_{r2}. The lower layer is characterized by electrical parameters σ_1 and σ

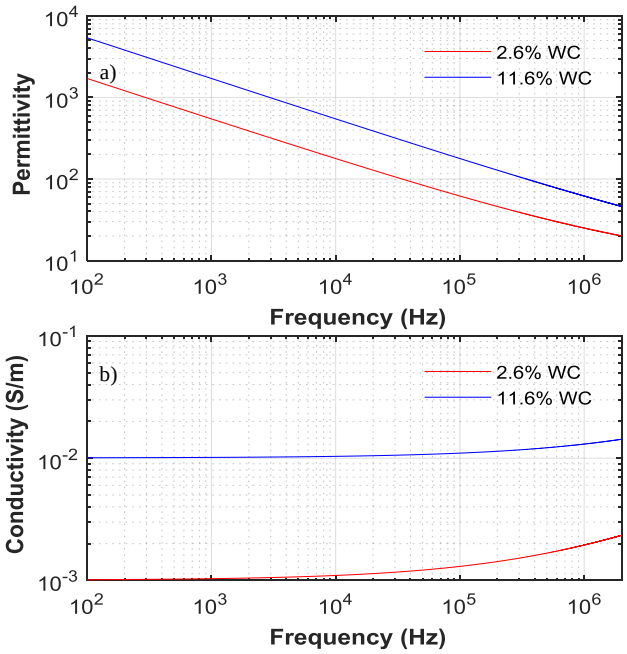

Fig.1 Frequency dependence of the soil's relative permittivity and conductivity for two different water content (WC) levels, 2.6% and 11.6%.

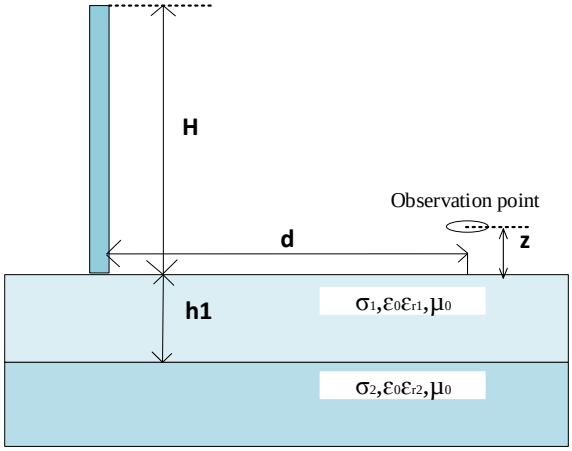

Fig. 2. Geometry for the calculation of lightning electromagnetic fields above a two-layer soil.

2.3 Electromagnetic Field Computation over a Horizontally Stratified Ground Considering a Frequency-Dependent Soil

In this study, we will use expressions derived initially by *Wait* [12]-[13] and *Hill and Wait* [49], which were suitably adapted for lightning electromagnetic field calculations by Cooray and co-workers (*Ming and Cooray* [14] and *Cooray and Cummins* [15]). For an overview of various methods to evaluate lightning electromagnetic fields, the reader can refer to [50]. Their validity has been tested versus full-wave approaches in several studies, e.g., *Shoory et al.* [16], [18].

The frequency-domain expressions for the vertical electric field, horizontal electric field and azimuthal

magnetic field above a two-layer soil are expressed as [50]:

$$E_z(d,z,jw) = E_{z,p}(d,z,jw)F_{str}(jw) \quad (5)$$

$$E_r(d,z,jw) = E_{r,p}(d,z,jw) - H_{j,p}(d,0,jw)F_{str}(jw)Z_{str}(jw) \quad (6)$$

$$H_j(d,z,jw) = H_{j,p}(d,z,jw)F_{str}(jw) \quad (7)$$

in which d is the horizontal distance to the observation point, z is the height of the observation point, the subscript p denotes that the field component is evaluated assuming a perfectly-conducting ground, F_{str} is the attenuation function accounting for the propagation effects, and Z_{str} is the ground surface impedance.

It is seen that, similar to the original Cooray-Rubinstein formula ([51]-[52]), the first term in (6) is the horizontal electric field at the observation point height above a perfectly conducting ground and the second term is the horizontal magnetic field on the ground surface, multiplied by the surface impedance of the ground Z_{str}. Note that the propagation effects of the magnetic field component ([53]-[54]) are considered in the calculation of the horizontal electric field (Equation (6)) in the present study.

The expression for the attenuation function ($Fstr$) of a stratified ground is given by

$$F_{str}(j\omega) = 1 - j\sqrt{\pi p_{str}}\, e^{-p_{str}}\, erfc(j\sqrt{p_{str}}) \quad (8)$$

in which the numerical distance p_{str} is defined as

$$p_{str} = -0.5\gamma_0 d\Delta_{str}^2 \quad (9)$$

Δ_{str} is the normalized surface impedance of the two-layer ground considering frequency-dependent soil parameters, given by

$$\Delta_{str} = \frac{Z_{str}(j\omega)}{\sqrt{(\mu_0/\varepsilon_0)}} \quad (10)$$

where

$$Z_{str} = \sqrt{\frac{\varepsilon_0}{\mu_0}} K_1 \frac{K_2 + K_1 \tanh(u_1 h_1)}{K_1 + K_2 \tanh(u_1 h_1)} \quad (11)$$

is the surface impedance of a two-layer soil, with

$$K_1 = \frac{u_1}{\sigma_1 + j\omega\varepsilon_0\varepsilon_{r1}} \quad (12)$$

$$K_2 = \frac{u_2}{\sigma_2 + j\omega\varepsilon_0\varepsilon_{r2}} \quad (13)$$

$$u_1 = \sqrt{\gamma_1^2 - \gamma_0^2} \quad (14)$$

and

$$u_2 = \sqrt{\gamma_2^2 - \gamma_0^2} \quad (15)$$

The propagation constants in each ground layer are given by

$$\gamma_1 = \sqrt{j\omega\mu_0(\sigma_1 + j\omega\varepsilon_0\varepsilon_{r1})} \quad (16)$$

and

$$\gamma_2 = \sqrt{j\omega\mu_0(\sigma_2 + j\omega\varepsilon_0\varepsilon_{r2})} \quad (17)$$

in which σ_1, σ_2, ε_{r1} and ε_{r2} are the frequency-dependent conductivities and permittivities of the top and lower layers. It is worth noting that the attenuation function F_{str} given by (8) does not consider the curvature of the earth since the considered observation points are within 100 km from the lightning channel.

2.4 Ground Parameters

The adopted values for water content used in the calculation of the electrical parameters of the ground are given in Table II. For the case of a constant-parameter soil model, the dielectric constants for the soil with 2.6% and 11.6% water content are set to ε_r = 5 and ε_r = 40, respectively. As can be seen from the Table II, four different cases are considered in the simulations:

- Case 1: homogeneous with 2.6% water content, corresponding to a DC conductivity of 0.001 S/m.
- Case 2: homogeneous with 11.6% water content, corresponding to a DC conductivity of 0.01 S/m.
- Case 3: two-layer soil with an upper layer of 2.6% and lower layer of 11.6% water content.
- Case 4: two-layer soil with an upper layer of 11.6% and lower layer of 2.6% water content.

3. Results and Analysis

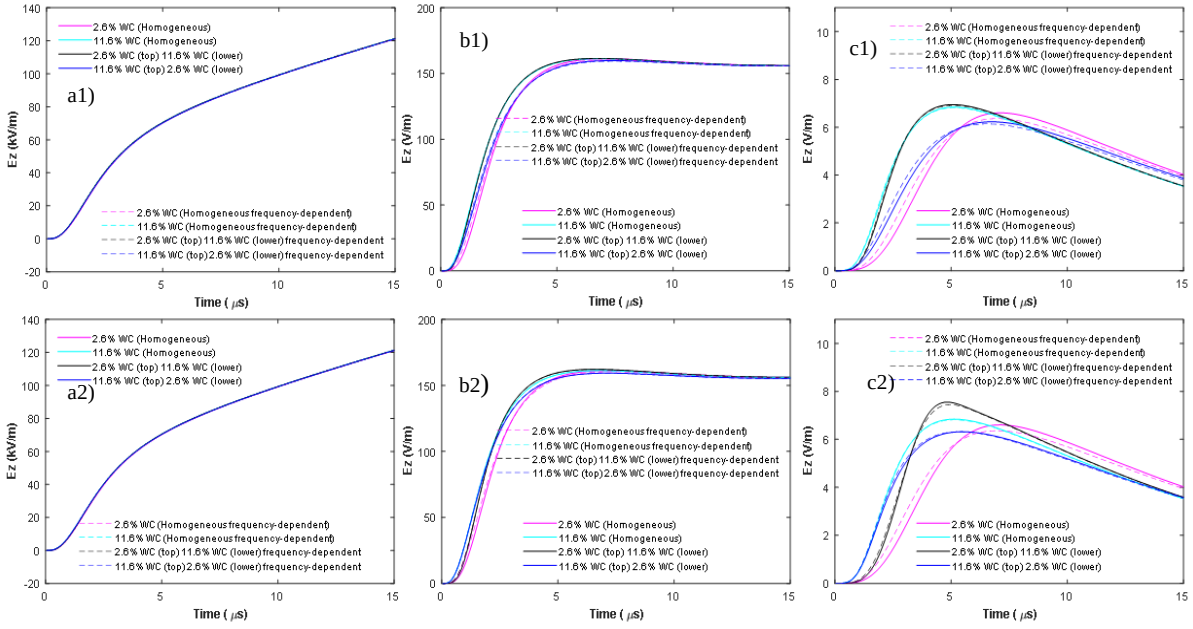

Fig.3 Vertical electric field (Ez) at 50 m (a1, a2), 5 km (b1, b2), and 100 km (c1, c2). First return stroke. The depth of the top layer is h1=2 m in the first row (a1, b1 and c1) and h1=10 m in the second row (a2, b2 and c2).

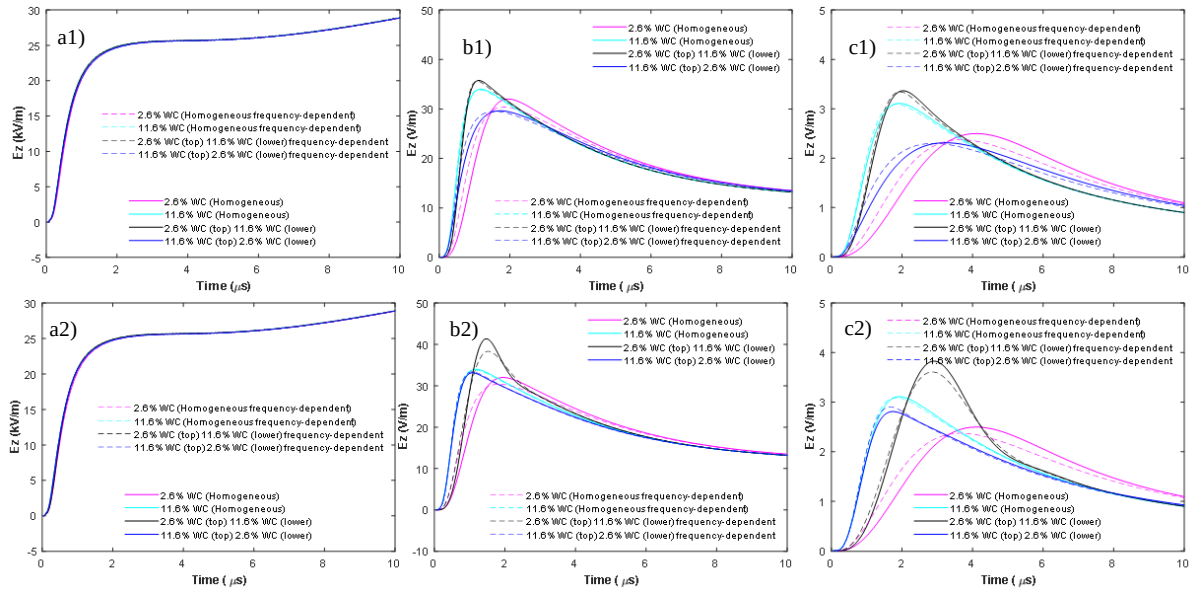

Fig.4 Vertical electric field (Ez) at 50 m (a1, a2), 5 km (b1, b2), and 100 km (c1, c2). Subsequent return stroke. The depth of the top layer is h1=2 m in the first row (a1, b1 and c1) and h1=10 m in the second row (a2, b2 and c2).

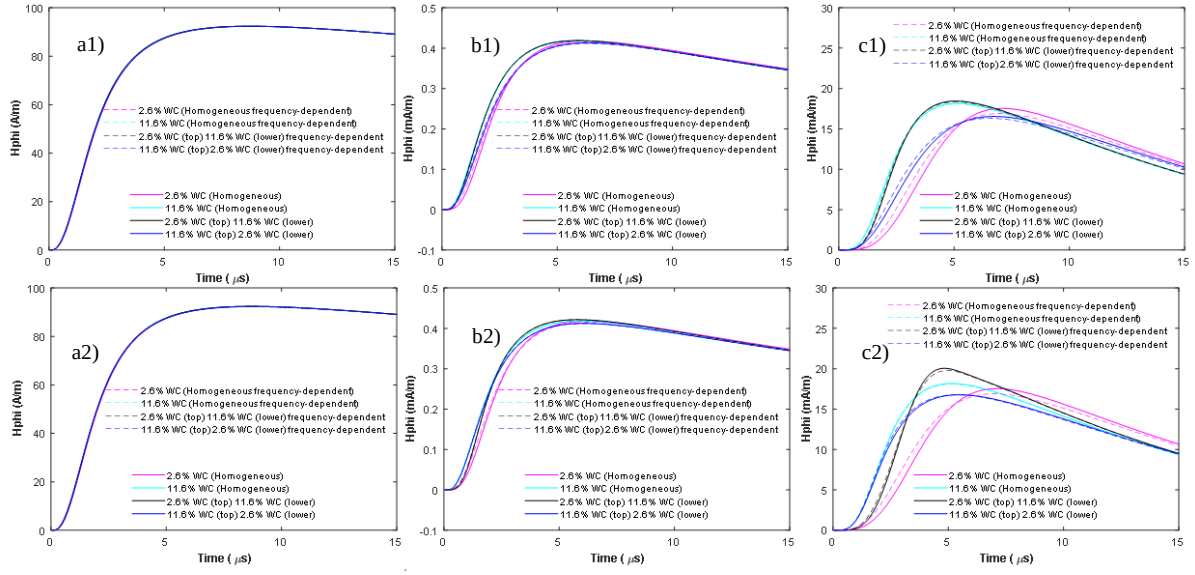

Fig.5 Azimuthal magnetic field (Hphi) at 50 m (a1, a2), 5 km (b1, b2), and 100 km (c1, c2). First return stroke. The depth of the top layer is h1=2 m in the first row (a1, b1 and c1) and h1=10 m in the second row (a2, b2 and c2).

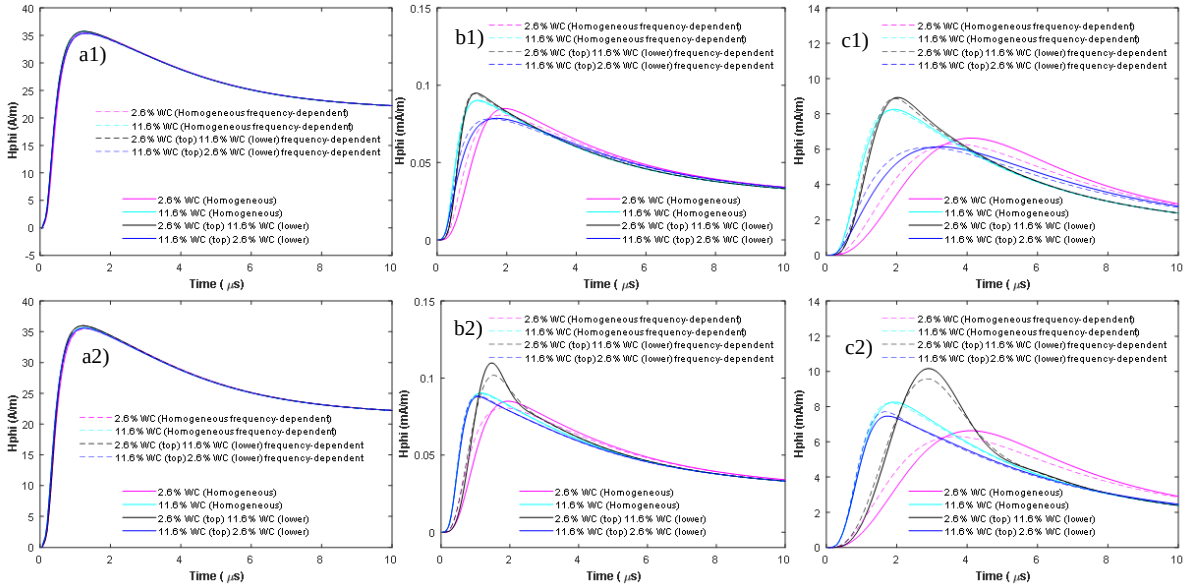

Fig.6 Azimuthal magnetic field (Hphi) at 50 m (a1, a2), 5 km (b1, b2), and 100 km (c1, c2). Subsquent return stroke. The depth of the top layer is h1=2 m in the first row (a1, b1 and c1) and h1=10 m in the second row (a2, b2 and c2).

3.1 Vertical Electric Field and Azimuthal Magnetic Field

Fig. 3 presents the numerical results for the vertical electric field radiated by a first return stroke at a distance of 50 m, 5 km, and 100 km from the channel, considering two different depths of the top layer, namely h1 = 2 m (a1, b1 and c1) and h1 = 10 m (a2, b2 and c2). Simulations corresponding to a constant conductivity and permittivity are presented in solid lines, while those obtained taking into account the frequency dependence of the electrical parameters of the soil are presented in dashed lines. Similar results are presented in Fig. 4 for a subsequent return stroke. In the same plots, we have also presented the results corresponding to the cases of a homogeneous (non-stratified) ground by extending the soil parameters of the upper layer to the rest of the ground under it. Figs. 5 and 6 present the corresponding results for the azimuthal magnetic fields.

It is shown that the vertical electric field and the azimuthal magnetic field at a close distance (a1 and a2 in Fig. 3 and Fig. 5) are virtually unaffected by either the soil heterogeneity or the frequency-dependent parameters. The simulated results are in agreement with [17] and [18], indicating that the assumption of a perfectly conducting ground is suitable to reproduce these field components at the considered close distance range. The impact of the soil on the considered field components becomes more significant at larger distances. At intermediate and far distances, the vertical electric field and the azimuthal magnetic field appear to be more markedly affected by the soil stratification than by its frequency dependence. Furthermore, compared to first return stroke fields, subsequent return stroke fields are more significantly affected by the soil stratification and frequency-dependence.

As discussed in [16], for the considered case of a two-layer ground with the top layer being characterized by a lower conductivity, the magnitude of the attenuation function (8) can become more than unity, causing an enhancement of the radiation field. The field peak, in this case, can even be larger than that corresponding to the case of a perfect ground.

3.2 Horizontal Electric Field

Fig. 7 and Fig. 8 present the horizontal electric field at 50 m, 5 km and 100 km. The observation point is set to 10 m above the ground surface, which is a typical height of overhead power distribution lines. The horizontal field in the vicinity of the lightning channel (50 m), in agreement with previous results (e.g., [17]-[19]), is not sensitive to the electrical characteristics of the ground. One can also see that, in agreement with Mimouni et al. [17], when the upper layer is less conductive, the early-time response of the horizontal electric field at distances of 5 km and 100 km is essentially determined by the upper layer, while its late-time response is governed by the lower, more conductive layer.

Fig. 9 presents the simulated horizontal electric field at 50 m near ground level (0.5 m). Compared to the simulated results at 10 m above the ground (a1 and a2 in Figs.7 and 8), it can be seen that the horizontal electric field at close distance and near ground level (0.5 m) is markedly affected by the soil stratification. It can also be seen from Fig. 9 that the horizontal field exhibits a noticeable negative excursion, as opposed to the field at the same distance but for an observation point located at a 10-m height (Fig. 8a). As discussed in Shoory et al. [18], the horizontal electric field (Equation (6)) consists of two terms. The first one is the contribution due to the elevation of the observation point above a perfect ground. The second term is the correction term accounting for the ground losses responsible for the conduction and displacement currents flowing into the ground. The former is of positive polarity and it increases with increasing height of the observation point above the ground. The latter, which is of negative polarity, on the other hand, is not dependent on the height of the observation point above the ground, and its absolute peak increases with the ground resistivity. For an observation point 10 m above the ground and at close range, the field is essentially dominated by the first term. When approaching the ground surface, the effect of the second term becomes more significant. The contribution of the second term becomes also dominant at intermediate and far distance ranges (i.e., 5 km and 100 km) regardless of the observation point height, resulting in a horizontal electric field of negative polarity, as can be seen in Figs. 7 and 8, panels b1, b2, c1, c2. The horizontal electric field is also more significantly affected by the soil stratification than by the frequency dependence of the soil's parameters. In agreement with [20], compared to the case of a homogeneous ground, the stratified ground results in significantly faster risetimes and falltimes for the horizontal electric field, characterized by an oscillatory behavior (see Fig. 8, panels b2 and c2).

As can be seen from Fig. 1b, the soil conductivity features an increase at high frequency, which is more pronounced for low-conducting soils. As a result of the frequency-dependence of the ground conductivity, the negative peak of the horizontal electric field is reduced compared to the case of a constant-parameter model. It can also be seen that the reduction in the negative field peak is more significant for subsequent return strokes than for the first return stroke. This can be explained by the fact that the subsequent return stroke current spectrum extends to higher frequencies compared to the first stroke.

In general, the simulation results reveal that the impact of the frequency-dependent soil on the electromagnetic field components is noticeable in a poorly-conducting ground (conductivity of 10^{-3} S/m or lower or, equivalently, for water content of 2 to 3%).

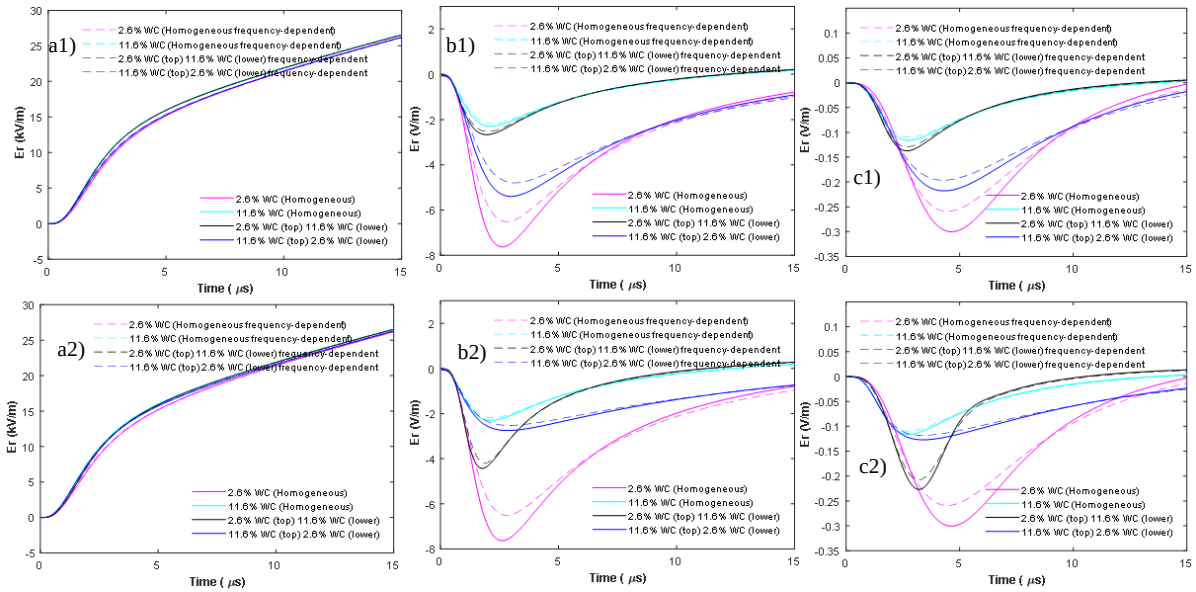

Fig.7 Horizontal electric field (Er) at 50 m (a1, a2), 5 km (b1, b2), and 100 km (c1, c2). First return stroke. The depth of the top layer is h1=2 m in the first row (a1, b1 and c1) and h1=10 m in the second row (a2, b2 and c2). The observation point was set to 10 m above the ground surface.

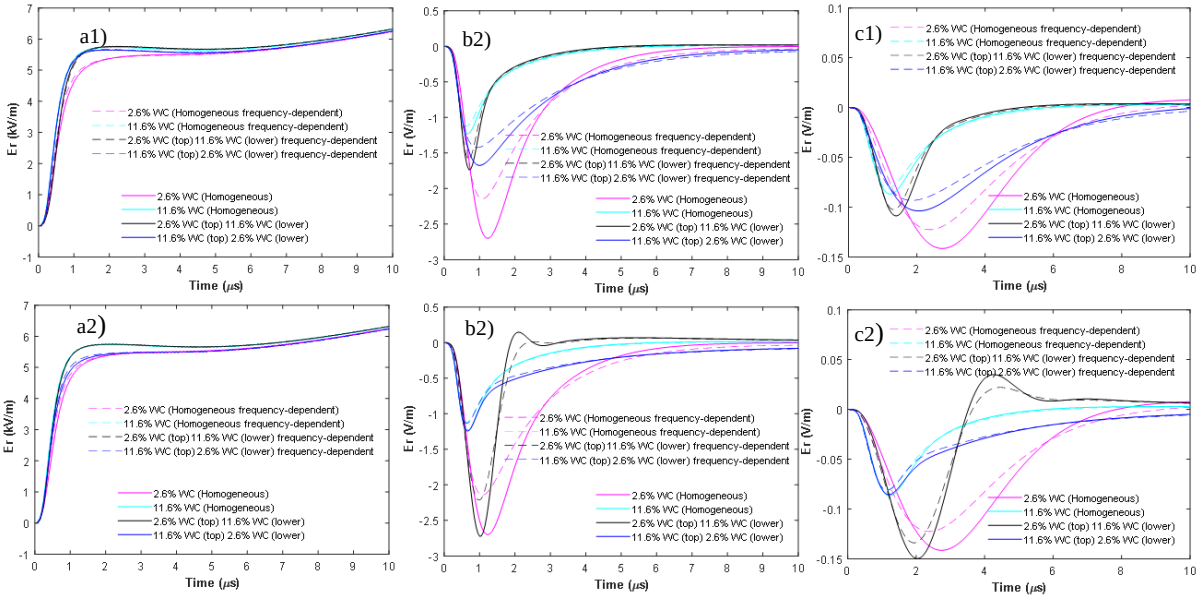

Fig. 8 Horizontal electric field (Er) at 50 m (a1, a2), 5 km (b1, b2), and 100 km (c1, c2). Subsquent return stroke. The depth of the top layer is h1=2 m in the first row (a1, b1 and c1) and h1=10 m in the second row (a2, b2 and c2). The observation point was set to 10 m above the ground surface.

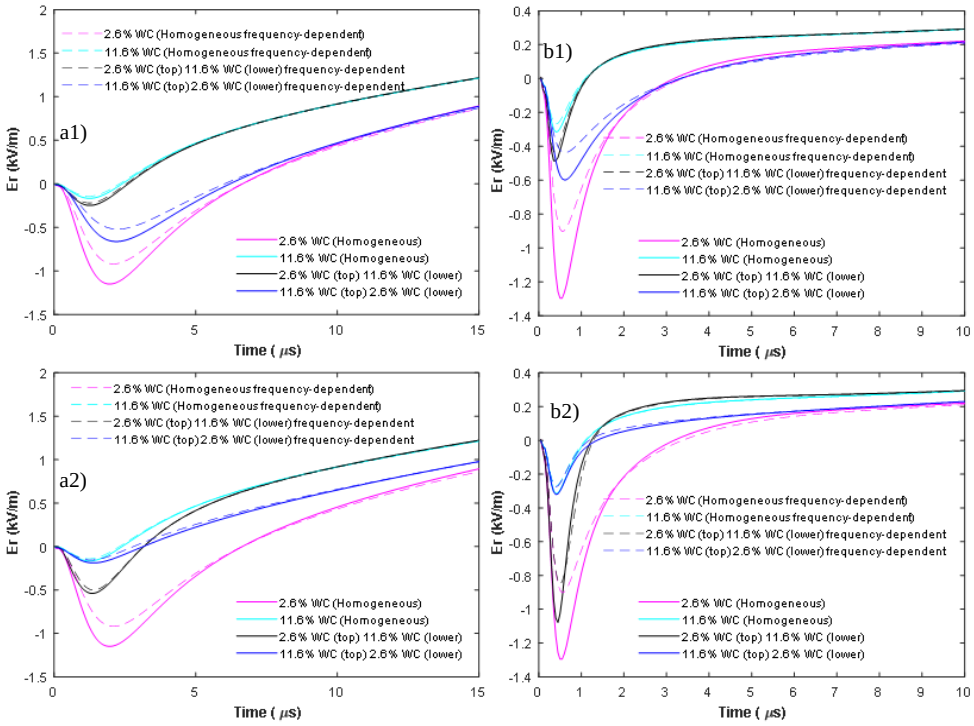

Fig. 9 Horizontal electric field (Er) at 50 m for the first return stroke (a1, a2) and subsquent return stroke (b1, b2). The depth of the top layer is h1=2 m in the first row (a1 and b1) and h1=10 m in the second row (a2 and b2). The observation point was set to 0.5 m above the ground surface.

TABLE III ELETROMAGNETIC FIELD PEAK VALUE AT 100 KM FOR CONSTANT SOIL PARAMETERS

		h1 = 2 m	h1 = 10 m	h1 = 2 m	h1 = 10 m	h1 = 2 m	h1 = 10 m
First RS	Case 1	6.6	5.9	37.0	37.0	17.5	17.5
	Case 2	6.9	6.8	11.8	11.8	18.2	18.2
	Case 3	7.0	7.6	12.7	17.1	18.4	20.0
	Case 4	6.2	6.3	29.4	15.4	16.5	16.8
Subsequent RS	Case 1	2.5	2.1	8.6	8.6	6.6	6.6
	Case 2	3.2	3.1	2.9	2.9	8.3	8.3
	Case 3	3.5	3.4	3.8	3.3	8.9	10.2
	Case 4	2.3	2.8	5.3	2.5	6.1	7.5
		Vertical electric field (V/m)		Horizontal electric field (mV/m)		Azimuthal magnetic field (mA/m)	

TABLE IV ELETROMAGNETIC FIELD 10-90% RISETIME AT 100 KM FOR CONSTANT SOIL PARAMETERS

		h1 = 2 m	h1 = 10 m	h1 = 2 m	h1 = 10 m	h1 = 2 m	h1 = 10 m
First RS	Case 1	3.5	3.8	7.2	7.2	3.5	3.5
	Case 2	2.4	2.4	7.2	7.2	2.4	2.4
	Case 3	2.2	2.6	6.9	6.0	2.3	2.2
	Case 4	3.4	2.5	8.1	10.3	3.4	2.6
Subsequent RS	Case 1	2.3	2.0	2.1	2.1	2.2	2.2
	Case 2	0.9	0.9	2.0	2.0	1.0	1.0
	Case 3	1.0	1.9	1.7	0.5	1.0	1.5
	Case 4	1.7	0.8	7.4	11.2	1.8	0.8
		Vertical electric field (μs)		Horizontal electric field (μs)		Azimuthal magnetic field (μs)	

TABLE V ELETROMAGNETIC FIELD PEAK VALUE AT 100 KM FOR FREQUENCY-DEPENDENT SOIL

		h1 = 2 m	h1 = 10 m	h1 = 2 m	h1 = 10 m	h1 = 2 m	h1 = 10 m
First RS	Case 1	6.4	6.4	31.5	31.5	16.9	16.9
	Case 2	6.8	6.8	11.3	11.3	18.1	18.1
	Case 3	6.9	7.5	12.2	16.4	18.3	19.8
	Case 4	6.1	6.3	25.3	13.4	16.3	16.8
Subsequent RS	Case 1	2.4	2.4	5.7	5.7	6.3	6.3
	Case 2	3.1	3.1	2.5	2.5	8.2	8.2
	Case 3	3.3	3.6	3.3	22.1	8.9	9.6
	Case 4	2.3	2.9	4.3	2.0	6.1	7.7
		Vertical electric field (V/m)		Horizontal electric field (mV/m)		Azimuthal magnetic field (mA/m)	

TABLE VI ELETROMAGNETIC FIELD 10-90% RISETIME AT 100 KM FOR FREQUENCY-DEPENDENT SOIL

		h1 = 2 m	h1 = 10 m	h1 = 2 m	h1 = 10 m	h1 = 2 m	h1 = 10 m
First RS	Case 1	3.4	3.4	7.6	7.6	3.4	3.4
	Case 2	2.5	2.5	7.3	7.3	2.4	2.4
	Case 3	2.3	2.3	7.0	6.1	2.3	2.3
	Case 4	3.2	2.5	8.5	10.6	3.2	2.5
Subsequent RS	Case 1	2.0	2.0	3.9	3.9	2.0	2.0
	Case 2	0.9	0.9	2.1	2.1	0.9	0.9
	Case 3	1.0	1.5	1.8	0.5	1.0	1.5
	Case 4	1.4	0.8	8.9	11.4	1.4	0.8
		Vertical electric field (μs)		Horizontal electric field (μs)		Azimuthal magnetic field (μs)	

Tables III and IV summarize the obtained values for the magnitude and 10-90% risetime of the vertical electric field, horizontal electric field and azimuthal magnetic field at 100 km for the different considered cases, assuming frequency-independent soil parameters. Tables V and VI present similar results but taking into account the frequency dependence of the soil parameters.

4. Comparison with Experimental Data

In this section, simultaneous measurements of current and distant vertical electric fields associated with rocket-triggered lightning flashes are used to analyze the effect of the soil stratification and the frequency dependence of the soil parameters.

4.1 Instrumentation and Data

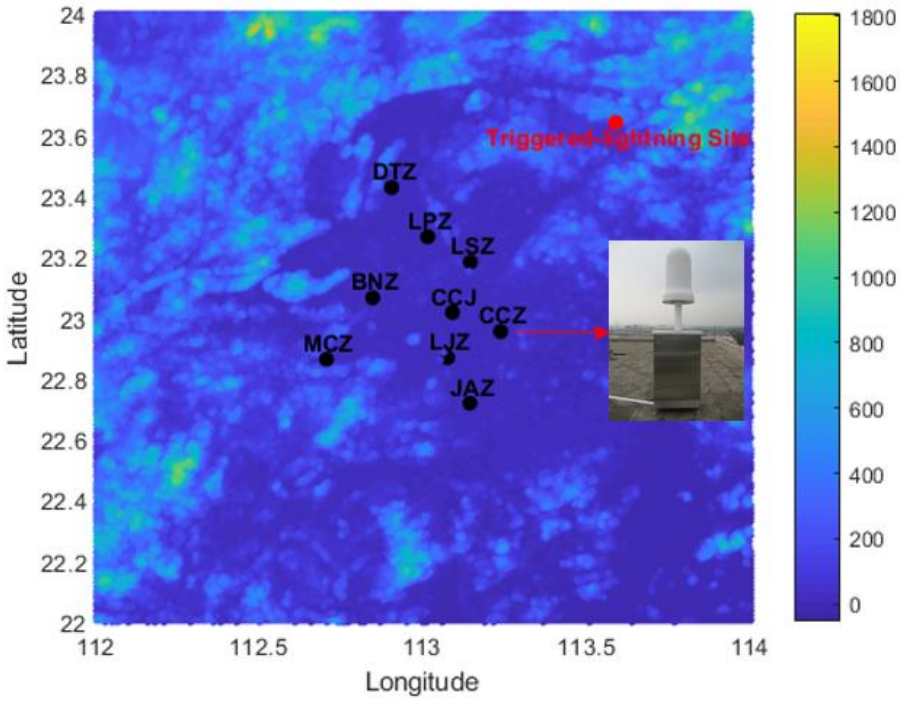

Fig.10 The topographic map of the sensors belonging to Foshan Total Lightning Location System (FTLLS, shown as black dots). The rocket-triggering lightning site is shown with a red dot. A picture of the sensor that was used for the comparison (station CCZ) is shown in the figure inset.

Fig. 10 presents the geographical distribution of the sensors belonging to the Foshan Three-Dimensional Lightning Location System (FTLLS). The rocket-triggering lightning site, located in Conghua, Guangdong, is also shown in the figure. FTLLS started its operation during the Summer of 2013. The network consists of nine stations. The shortest and farthest distances separating each station to the lightning triggering site are 69 km and 126 km. The propagation path is over land and mainly over flat ground. The topographic map of the region of interest is based on data from the global digital elevation model (GDEM V2). We will use the electric field data obtained at the station CCZ of the network, which is 85 km away from the triggering site. Detailed information about the triggered-lightning site (GCOELD) is available in *Zhang* et al. [55].

Wideband electric field measuring systems with a 3 dB bandwidth from 160 Hz to 500 kHz are employed to measure the lightning electromagnetic fields at each station. The systems are equipped with analog integrators with a 1-ms decay time constant. Electric field signals produced by triggered lightning discharges were digitized with a 10-MS/s sampling rate. Detailed information on the experimental setup can be found in [56]-[57].

Fig. 11 presents the measured current waveform associated with one of the return strokes of flash F20140603 recorded on June 3, 2014, at 6:43 AM (local time). In the same figure, the analytical representation of the measured current using Heidler's functions is also shown. The values of the parameters were set to $I_{01} = 16.0\ kA$, $\tau_{11} = 0.501\ \mu s$, $\tau_{12} = 9.6\ \mu s$, $n_1 = 5$, $I_{02} = 5.6\ kA$, $\tau_{21} = 10.0\ \mu s$, $\tau_{22} = 7\ \mu s$ and $n_2 = 3$. The analytical current was used as an input in the numerical simulations. The return stroke model and the adopted parameters are the same as in Section II.A.

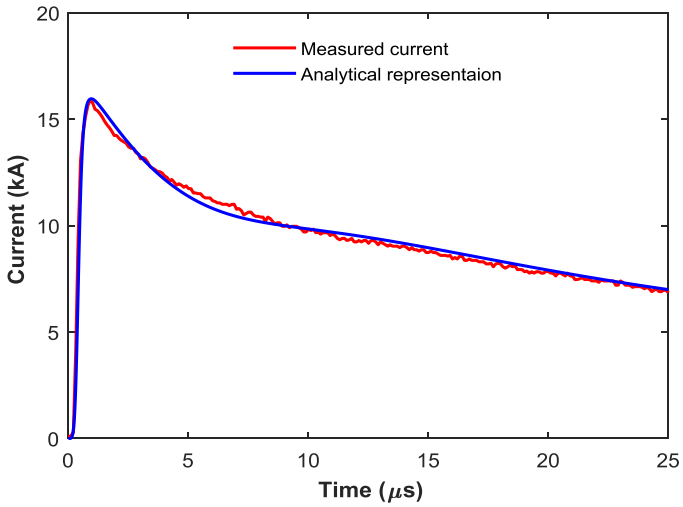

Fig.11 Measured current waveform associated with a return stoke of the triggered-lightning flash F20140603 recorded on June 3, 2014, at 6:43 AM (local time) (solid red line) and its analytical representation using Heidler's functions (solid blue line).

4.2 Vertical Electric Field Simulation

The simulation results for different soil conditions are presented in Fig. 12. Since no information on the characteristics of the soil was available, for each case (homogeneous, stratified, frequency-independent and frequency-dependent), the soil parameters were chosen to obtain the best match with experimental results.

As discussed in [37], it can be seen that, compared to the homogeneous ground case, the computed electric field waveform for the case of a two-layer soil follows to a much better extent the experimental waveform, with the exception of the hump that appears some 10 μs after the onset of the return stroke field, which is not reproduced by any of the models. The frequency-dependence of the soil affects slightly the early-time response of the field. However, the late-time response of the field is essentially determined by the soil stratification.

A detailed comparison between calculated and measured waveforms of return strokes at seven stations can be found in [37].

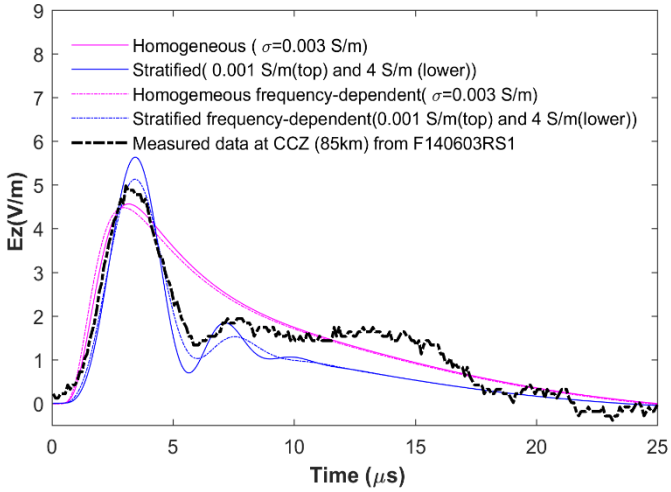

Fig.12 Vertical electric field associated with the return stroke current of Fig. 11, measured at station CCZ, at a distance of 85 km from the lightning channel. Simulated results for different soil models are also presented in the same plot.

5. Conclusions

We presented an analysis of lightning electromagnetic fields at different distances taking into account the soil stratification and the frequency dependence of its electrical parameters. The return stroke channel was modeled using the MTLE model, assuming a current decay constant $\lambda = 2$ km and a return stroke speed $v = 1.5\times10^8$ m/s. Two current waveforms corresponding to typical first and subsequent return strokes were considered for the analysis. Different cases for the soil (homogeneous, 2-layer, frequency-dependent/constant electrical parameters) were considered. The analysis was carried out considering different distance ranges: close (50 m), intermediate (5 km) and distant (100 km). The obtained results confirm that the vertical electric field and the azimuthal magnetic field at close range can be evaluated assuming the ground as a perfectly conducting plane. On the other hand, the horizontal electric field is found to be very sensitive to the ground stratification for all the considered distance ranges. However, at close range, the impact of the soil becomes less significant for observation points that are located at heights of 10 m above ground or higher. It was shown that the three field components, the vertical electric field, the horizontal electric field and the azimuthal magnetic field, are affected more markedly by the soil stratification than by the frequency dependence of its electrical parameters, especially for intermediate and distant ranges (i.e., 5 km and 100 km). Furthermore, the subsequent return stroke fields were more significantly affected by the soil stratification and frequency-dependence compared to the first return stroke fields. The impact of the frequency-dependent soil parameters on the considered field components was more noticeable in a poorly conducting soil compared to a good conducting soil.

We presented also a comparison between simulation results with simultaneous measurements of current and distant vertical electric fields associated with rocket-triggered lightning flashes. It was shown that the computed vertical electric field waveform for the case of a two-layer soil (compared to the homogeneous ground model) follows to a much better extent the corresponding experimental waveforms. The frequency-dependence of the soil affects slightly the early-time response of the field. However, the late-time response of the field is essentially determined by the soil stratification.

6. Acknowledgment

This research was supported by the Swiss National Science Foundation (Project No. 200021_147058), Natural Science Foundation of China under Grant 51877155 and 51807144, and the China Scholarship Council (CSC). The authors wish to express their gratitude to all the members of Guangzhou Field Experiment Site for Triggered Lightning at Conghua in Guangdong Province.

7. References

[1] K.L. Cummins, M.J. Murphy, E.A. Bardo, W.L. Hiscox, R. B. Pyle, and A.E. Pifer, A Combined TOA/MDF Technology Upgrade of the U.S. National Lightning Detection Network, J. Geophys. Res.,vol.103, no.D8, pp.9035–9044, 1998.

[2] Taylor, C. D., R. S. Satterwhite, and C. W. Harrison, The response of a terminated two- wire transmission line excited by a nonuniform electromagneticfield, IEEE Trans. Antennas Propag., vol. 13(6), pp. 987–989, 1965.

[3] Agrawal, A. K., H. J. Price, and S. H. Gurbaxani, Transient response of multiconductor transmission lines excited by a nonuniform electromagnetic field, IEEE Trans. Electromagn. Compat., vol. 22(2), pp. 119–129, 1980.

[4] Rachidi, F. , Formulation of the field- to- transmission line coupling equations in terms of magnetic excitation fields, IEEE Trans. Electromagn. Compat., vol. 35(3), pp. 404–407, 1993.

[5] Rachidi, F., and S. Tkatchenko (Eds.) (2008), Electromagnetic Field Interaction with Transmission Lines: From Classical Theory to HF Radiation Effects, WIT Press, Southampton, U. K., doi:10.2495/978-1-84564-063-7.

[6] V. Cooray, F. Rachidi, and M. Rubinstein, Formulation of the Field-to-Transmission Line Coupling Equations in Terms of Scalar and Vector Potentials, IEEE Trans. Electromagn. Compat., vol. 59, no. 5, pp. 1–6, 2017.

[7] A. Piantini, Extension of the Rusck Model for calculating lightning-induced voltages on overhead lines considering the soil electrical parameters, IEEE Trans Electromagn. Compat.,vol. 59, no.1, pp. 154-168, 2017.

[8] V. Cooray, The lightning flash, in Power and Energy Series, vol. 34, London, U.K.: IET, 2003.

[9] V. Cooray, On the accuracy of several approximate theories used in quantifying the propagation effects on lightning generated electromagnetic fields, IEEE Trans. Antennas Propag., vol. 56, no. 7, pp. 1960–1967, Jul. 2008.

[10] V. Cooray, Propagation on effects due to finitely conducting ground on lightning-generated magnetic fields evaluated using Sommerfeld's integrals, IEEE Trans. Electromagn. Compat., vol. 51, no. 3, pp. 526–531, Aug. 2009.

[11] V. Cooray and H. Perez, Propagation effects on the first return stroke radiation fields: Homogenous paths and mixed two section paths, presented at 22nd International Conference on Lightning Protection, Budapest, Hungary, 1994, Paper R: 1a-06.

[12] J. R. Wait, Radiation from a vertical electric dipole over a stratified ground, I.R.E. Transactions on Antennas and Propagation, vol. 1, pp. 9–11, 1953.

[13] J. R. Wait, On the theory of transient electromagnetic sounding over a stratified earth, Canadian Journal of Physics, vol. 50, pp. 1055–1061, June 1972.

[14] Y. Ming and V. Cooray, Electromagnetic radiation fields generated by lightning return strokes over a stratified ground, in 22nd International Conference on Lightning Protection (ICLP), Budapest, pp. R1c-05, 1994.

[15] V. Cooray and K. L. Cummins, Propagation effects caused by stratified ground on electromagnetic fields of return strokes, presented at the 20th International Lightning Detection Conference & 2nd International Lightning Meteorology Conference, Tucson, Arizona, USA, 2008.

[16] A. Shoory, A. Mimouni, F. Rachidi, et al.,Validity of simplified approaches for the evaluation of lightning electromagnetic fields above a horizontally stratified ground, IEEE Trans. Electromagn. Compat., vol. 52, no. 3, pp. 657–663, Apr. 2010.

[17] A. Mimouni, F. Rachidi, and M. Rubinstein, Electromagnetic Fields of a Lightning Return Stroke in Presence of a Stratified Ground, IEEE Trans. Electromagn. Compat., vol. 56, no. 2, pp.413-418, 2010.

[18] Shoory, A., F. Rachidi, F. Delfino, R. Procopio, and M. Rossi , Lightning electromagnetic radiation over a stratified conducting ground: 2. Validity of simplified approaches, J. Geophys. Res., vol.116, D11115, 2011.

[19] F. Delfino, R. Procopio, M. Rossi, A. Shoory, F. Rachidi, The effect of a horizontally stratified ground on lightning electromagnetic fields, 2010 IEEE International Symposium on Electromagnetic Compatibility

[20] A. Shoory, A. Mimouni, F. Rachidi, V. Cooray and M. Rubinstein, Lightning horizontal electric fields above a two-layer ground, in International Conference on Lightning Protection (ICLP), Cagliari, Italy, 2010, pp. 1285, 1–1285, 5.

[21] J. Paknahad, K. Sheshyekani, F. Rachidi, and M. Paolone, Lightning electromagnetic fields and their induced currents on buried cables. Part II: The effect of a horizontally stratified ground, IEEE Trans. Electromagn. Compat., vol. 56, no. 5, pp. 1146−1154, Oct. 2014.

[22] J. Paknahad, K. Sheshyekani, F. Rachidi, Lightning electromagnetic fields and their induced currents on buried cables. Part I: The effect of an ocean–land mixed propagation path, IEEE Trans. Electromagn. Compat., vol. 56, no. 5, pp. 1137−1145, Oct. 2014.

[23] Q. Zhang, D. Li, Y. Zhang, J. Gao, and Z. Wang, On the accuracy of Wait's formula along a mixed propagation path within 1 km from the lightning channel, IEEE Trans. Electromagn. Compat., vol. 54, no. 5, pp. 1042–1047, Oct. 2012.

[24] Li, D., Rubinstein, M., Rachidi, F., Diendorfer, G., Schulz, W., & Lu, G., Location accuracy evaluation of ToA-based lightning location systems over mountainous terrain, J. Geophys. Res., vol. 122, pp. 11,760–11,775. 2017.

[25] Delfino, F., R. Procopio, M. Rossi, and F. Rachidi, Influence of frequency-dependent soil electrical parameters on the evaluation of lightning electromagnetic fields in air and underground, J. Geophys. Res., vol.114, D11113, 2009.

[26] M. Zhou, J. Wang, L. Cai, Y. Fan, and Z. Zheng, Laboratory investigations on factors affecting soil electrical resistivity and the measurement, IEEE Transactions on Industry Applications, vol. 51, no. 6, Nov. 2015.

[27] D. Cavka, N. Mora, and F. Rachidi, A comparison of frequency dependent soil models: Application to the analysis of grounding systems, IEEE Trans. Electromagn. Compat., vol. 56, no. 1, pp. 177–187, Feb. 2014.

[28] F. H. Silveira, A. D. Conti, S. Visacro, Evaluation of Lightning-Induced Voltages over Lossy Ground with Frequency-dependent Soil Parameters," in. Int. Conf. Lightning Protection, 2014.

[29] M. Akbari, K.Sheshyekani, A. Pirayesh, F. Rachidi, M. Paolone, A. Borghetti, and C. A. Nucci, Evaluation of lightning electromagnetic fields and their induced voltages on overhead lines considering the frequency dependence of soil electrical parameters, IEEE Trans. Electromagn. Compat., vol. 55, no. 6, pp.1210-1219, 2013.

[30] Silveira, F. H., Visacro, S., Alipio, R., & De Conti, A., Lightning-Induced Voltages Over Lossy Ground: The Effect of Frequency Dependence of Electrical Parameters of Soil, IEEE Trans. Electromagn. Compat., 56(5), 1129–1136, 2014.

[31] K. Sheshyekani and J. Paknahad, Lightning Electromagnetic Fields and Their Induced Voltages on Overhead Lines: The Effect of a Horizontally Stratified Ground, IEEE Trans. Power Del., 30(1), 290–298, 2015.

[32] M. Akbari, K.Sheshyekani, M. R. Alemi, The Effect of Frequency Dependence of Soil Electrical Parameters on the Lightning Performance of Grounding Systems, IEEE Trans. Electromagn. Compat., vol. 55, no. 4, pp.739-746, 2013.

[33] S. Visacro, R. Alipio, M. H. Murta Vale, and C. Pereira,The response of grounding electrodes to lightning currents: The effect of frequencydependent soil resistivity and permittivity, IEEE Trans. Electromagn. Compat., vol. 53, no. 2, pp. 401–406, May 2011.

[34] S. Visacro and R. Alipio, Frequency dependence of soil parameters: Experimental results, predicting formula and influence on the lightning response of grounding electrodes, IEEE Trans.Power Del.,vol.27,no.2, pp. 927–935, Apr. 2012.

[35] Q. Zhang, T. Ji, and W. Hou, Effect of frequency-dependent soil on the propagation of electromagnetic fields radiated by subsequent lightning strike to tall objects, IEEE Trans. Electromagn. Compat., vol. 57, no. 1, pp.1210-1219, 2015.

[36] J. Paknahad, K. Sheshyekani, F. Rachidi, M. Paolone, and A. Mimouni, Evaluation of lightning-induced currents on cables buried in a Lossy dispersive ground, IEEE Trans. Electromagn. Compat., vol. 56, pp. 1522-1529, 2014.

[37] Q. Li, J. Wang, F. Rachidi, M. Rubinstein, A.Sunjerga, L. Cai, M. Zhou, Importance of Taking into Account the Soil Stratification in Reproducing the Late Time Features of Distant Field Radiated by Lightning, IEEE Trans. Electromagn. Compat., vol.61, no.3, pp.935-944, 2019.

[38] Q. Li, M. Rubinstein, J. Wang, L. Cai, M. Zhou, F.Rachidi, Distant Electric Fields from Lightning Return Strokes: Influence of Soil Stratification and Frequency-Dependent Parameters, 34th International Conference on Lightning Protection ICLP, Rzeszov, Poland, September 2-7, 2018.

[39] C. A. Nucci, C. Mazzetti, F. Rachidi, and M. Ianoz, On lightning return stroke models for LEMP calculations, presented at the 19th Int. Conf. Lightning Protection, Graz, Austria, 1988.

[40] F. Rachidi and C. A. Nucci, On the Master, Uman, Lin, Standler and the modified transmission line lightning return stroke current models, J. Geophys. Res., vol. 95, pp. 20389–20393, 1990.

[41] F. Heidler, Traveling current source model for LEMP calculation, in Proc. 6th Int. Zurich Symp. Electromagn. Compat., 1985, pp. 157–162.

[42] F. Rachidi, W. Janischewskyj, A. M. Hussein, C. A. Nucci, S. Guerrieri, B. Kordi, and J. Chang, Current and Electromagnetic Field Associated With Lightning–Return Strokes to Tall Towers, IEEE Trans. Electromagn. Compat., vol. 43, no. 3, pp.356-367, 2001.

[43] J. H. Scott, R. D. Carroll, and D. R. Cunningham, Dielectric constant and electrical conductivity of moist rock from laboratory measurements, Sensor and Simulation Note 116, Kirtland AFB, NM, Aug. 1964.

[44] J. H. Scott. (1966, May). Electrical and magnetic properties of rock and soil, Theoretical Notes, Note 18, U.S. Geological Survey [Online]. Available: https://www.ece.unm.edu/summa/notes/Theoretical.html

[45] J. H. Scott, D. Carroll, and D. R. Cunningham, Dielectric constant and electrical conductivity measurements of moist rock: A new laboratory method, J. Geophys. Res., vol. 72, no. 20, pp. 5101–5115, 1967.

[46] M. A. Messier, The propagation of an electromagnetic impulse through soil: Influence of frequency dependent parameters, Mission Res. Corp., Santa Barbara, CA, USA, Tech. Rep. MRC-N-415, 1980.

[47] M. Messier, Another soil conductivity model, internal rep., JAYCOR, Santa Barbara, CA, 1985.

[48] L. Grcev, High frequency grounding, in Lightning Protection, V. Cooray, Ed. London,, U.K.: IET, 2010, Ch. 10, pp. 503–529.

[49] D. A. Hill and J. R. Wait, HF radio wave transmission over sea ice and remote sensing possibilities, Geoscience and Remote Sensing, IEEE Transactions on, vol. GE-19, pp. 204–209, 1981.

[50] A. Shoory, F. Rachidi, V. Cooray, Propagation effects on electromagnetic fields generated by lightning return strokes: Review of simplified formulas and their validity assessment, Chapter 12 of "Lightning Electromagnetics", IET, pp. 485-513, 2012.

[51] V. Cooray, Horizontal fields generated by return strokes, Radio Science, vol. 27, pp. 529-537, 1992.

[52] Rubinstein, M., An approximate formula for the calculation of the horizontal electric field from lightning at close, intermediate, and long ranges, IEEE Trans. Electromagn. Compat., vol.38(3), pp.531–535,1996.

[53] Vernon Cooray, Horizontal Electric Field Above and Underground Produced by Lightning Flashes, IEEE Trans. Electromagn. Compat., vol. 52, no. 4, pp.936-943, 2010.

[54] M. Aoki, Y. Baba, and V. A. Rakov, FDTD simulation of LEMP propagation over lossy ground, J. Geophys. Res., vol. 120, doi:10.1002/2015JD023245, Aug. 2015.

[55] Y. J. Zhang, Experiments of artificially triggered lightning and its application in Conghua, Guangdong, China, Atmospheric Res., vol. 117, pp. 330–343, 2012.

[56] L. Cai, X. Zou, J.Wang, Q. Li, M. Zhou, Y. Fan, The Foshan Total Lightning Location System in China and Its Initial Operation Results, Atmosphere, vol.10(3), 149; 2019.

[57] J. Wang, Q. Li, L. Cai, M. Zhou, Y. Fan, J. Xiao, A. Sunjerga, Multiple-Station Measurements of a Return-Stroke Electric Field From Rocket-Triggered Lightning at Distances of 68–126 km, IEEE Trans. Electromagn. Compat, vol.51(2), pp. 440-448, Apr. 2019.